

CONF-9710193--

BNL-66423

RECEIVED  
JUN 09 1999  
OSTI

## Search for nuclei containing two strange quarks

Morgan May<sup>a,\*</sup>

<sup>a</sup>Physics Department, Brookhaven National Laboratory, Upton, NY 11973, USA

This paper discusses a search for nuclei containing two strange quarks performed at Brookhaven National Laboratory. The goals and approach of experiment E885 are reviewed. Preliminary missing mass spectra for a subset of the data are presented, showing sensitivity for  $\Xi$  hypernuclei and H particle searches. Existence of an angular correlation between pions in the sequential decay of  $\Lambda\Lambda$  hypernuclei is suggested on theoretical grounds.

### 1. INTRODUCTION

We would like to understand the state of matter that results when a nucleus contains two strange quarks. The terms  $\Lambda\Lambda$  and  $\Xi$  hypernuclei imply a structure in which the strange quarks are bound within hyperons; however, prior to conclusive discovery and study, it is not certain that this will be the case. The goal of experiments is to find these objects and determine their structure.

$\Lambda\Lambda$  and  $\Xi$  hypernuclei are basic to the understanding of the H particle [1], strangelets [2] and strange quark matter [3]. Predictions for these exotic forms of matter containing 3 flavors are based on symmetry, the Pauli principle, and the nature of the color-magnetic interaction.

The H particle is the simplest strangelet. If the H is deeply bound, two  $\Lambda$  particles in a hypernucleus will merge to form it. In any case, the presence of the H, even as an unbound resonance, will alter the structure of  $\Lambda\Lambda$  and  $\Xi$  hypernuclei.

Experiments at the Brookhaven Alternating Gradient Synchrotron (AGS) now have available to them beams of  $K^-$  two orders of magnitude more intense than used in previous searches [4]. Both AGS E885 [5] which will be the primary focus of this paper and AGS E906 [6], which is discussed in these proceedings by Fukuda, will have integrated fluxes in excess of  $10^{12} K^-$ .

### 2. EXPERIMENT 885 GOALS AND APPROACH

The primary goals of E885 are to search for:

1.  $\Lambda\Lambda$  hypernuclei produced by stopped  $\Xi^-$



\*This work has been supported by the United States Department of Energy under contract No. DE-AC02-98CH10886.

MASTER

DISTRIBUTION OF THIS DOCUMENT IS UNLIMITED

## **DISCLAIMER**

**This report was prepared as an account of work sponsored by an agency of the United States Government. Neither the United States Government nor any agency thereof, nor any of their employees, make any warranty, express or implied, or assumes any legal liability or responsibility for the accuracy, completeness, or usefulness of any information, apparatus, product, or process disclosed, or represents that its use would not infringe privately owned rights. Reference herein to any specific commercial product, process, or service by trade name, trademark, manufacturer, or otherwise does not necessarily constitute or imply its endorsement, recommendation, or favoring by the United States Government or any agency thereof. The views and opinions of authors expressed herein do not necessarily state or reflect those of the United States Government or any agency thereof.**

## **DISCLAIMER**

**Portions of this document may be illegible in electronic image products. Images are produced from the best available original document.**

When formed on a free proton in the reaction



the  $\Xi^-$  is very energetic ( $p_{\Xi^-} = 0.5 \text{ GeV}/c$  for  $p_{K^-} = 1.8 \text{ GeV}/c$ ) and is unlikely to stop in the target. When the reaction takes place on a proton bound in a nucleus, very slow  $\Xi^-$  can be produced due to the Fermi motion. The  $\Xi^-$  can then be stopped and be captured at rest by another  $^{12}\text{C}$  nucleus in the target (reaction 1). A diamond target was used for most of the data taking, since it gives the maximum density and therefore stopping power for a light element. Fig. 1 is a schematic view of the target area. The target is surrounded by a scintillating fiber array to detect the decay products of the double hypernucleus.

$\Xi^-$  which are likely to stop in the target are selected in the analysis by a restriction on the momentum of the  $K^+$ ; this has been studied by a Monte Carlo calculation of quasifree  $\Xi^-$  production which has been checked by comparison with KEK emulsion data [7]. Of course, the slowest  $\Xi^-$ s correspond to the fastest  $K^+$ s.

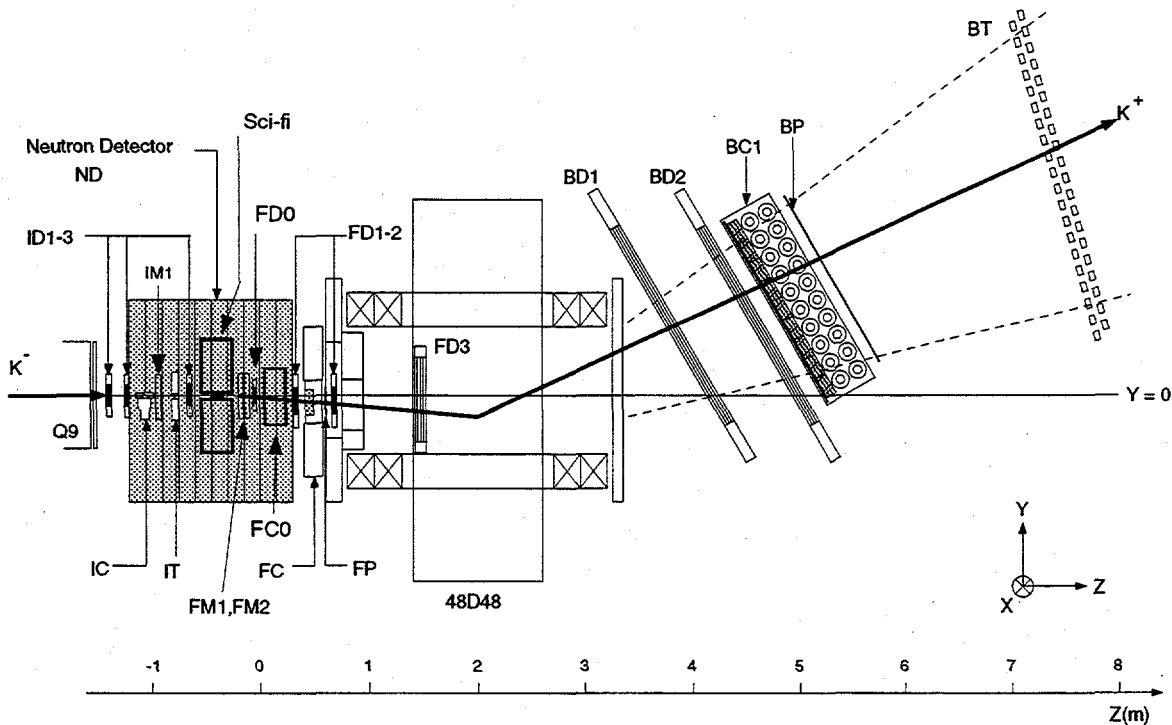


Figure 2. Apparatus of Experiment 885. Drift chambers ID1-3 and gas microstrip chamber IM1 determine the incoming  $K^-$  trajectory and are combined with upstream hodoscope data to determine the  $K^-$  momentum. Drift chambers FD1-3, BD1,2 and microstrip chambers FM1,2 determine the  $K^+$  momentum from deflection in spectrometer magnet 48D48. Scintillators IT and BT determine  $K^+$  time-of-flight. Hodoscopes FP and BP define the limits of the spectrometer acceptance. Aerogel Cherenkov counters IC1, FC and BC reject pions. High density aerogel counter FC0 rejects protons. Scintillating fiber array Sci-fi and neutron time-of-flight array ND surround the target.

### 3. EXPERIMENTAL DETAILS

Fig. 2 shows the apparatus. The same beam and spectrometer are also used for the  $\Lambda\Lambda$  hypernucleus search E906 discussed by Fukuda in these proceedings. The  $K^-$  beam is momentum analyzed using the chambers ID1-3 and a hodoscope and spectrometer not shown in the figure. The beam typically contained one  $\pi^-$  for each  $K^-$  with  $10^6$   $K^-$  in a pulse repeated every 3 seconds.

The diamond target weighs 140 gms and is  $5 \times 1 \times 8$  cm in extent. It was fabricated by closely packing  $1 \times 1 \times \approx 0.1$  cm blocks of industrial diamond made by a vapor deposition process. A density of  $\rho = 3.3$  gm/cm<sup>3</sup> was achieved, 93% of the density of single-crystal diamond.

A 48D48 dipole magnet flanked by drift chambers FD0-3 and BD1,2 momentum analyzes the  $K^+$  ( $p_{K^+} \approx 1.4$  GeV/c). Suppression of the  $\pi^- + p \rightarrow \Sigma^- + K^+$  background requires  $\pi^-/K^-$  discrimination accomplished by using time-of-flight and an aerogel Cherenkov counter IC. Aerogel Cherenkov counters FC and BC distinguish the  $\pi^+$  from  $K^+$ .

Protons resulting from ( $K^-, p$ ) elastic and inelastic scattering are the most serious problem at the trigger level. Offline, secondary mass constraints determined from time-of-flight and momentum analysis result in good  $K^+/p$  separation. Online, a second level trigger accomplishes roughly same end using a memory lookup table to impose cuts based on an FD3  $\times$  BT momentum matrix and IT-BT time-of-flight. For further trigger level proton rejection, an aerogel Cherenkov counter FC0 selects outgoing  $K^+$  for  $p_K > 0.89$  GeV/c and rejects protons with  $p_p < 1.84$  GeV/c. It uses a radiator with an index of refraction  $n=1.112$  especially fabricated for this experiment; formerly liquid  $H_2$  was the only way to achieve a comparable index. These strategies reduced the trigger rate sufficiently to permit writing most ( $K^-, K^+$ ) events to tape.

For a subset of events, scintillating fiber data was also recorded. A special level 1 trigger which initiated the readout of the scintillating fiber data included a multiplicity requirement on the hodoscope H (Fig. 1) and an FP-BT matrix to enrich the  $p_{K^+}$  region for which the associated  $\Xi^-$  is likely to stop.

Missing mass is determined by measurement of  $p_{K^-}$  and  $p_{K^+}$ ; resolution of 7 MeV FWHM was achieved for thin targets for  $\Xi^-$  production on free protons (reaction 5). Resolution for  $\Xi$  hypernuclei (reaction 2) is 50% broader due to kinematic effects.

Walls of thick, highly segmented scintillator ND on either side of the target measure neutron energy by time-of-flight; the neutron energy resolution is 1.5 MeV at 15 MeV.

The experiment had an integrated flux of  $8 \times 10^{11}$   $K^-$  on the diamond target. After reduction, 413,000 tagged  $K^+$  events (mainly  $\Xi$ ) survived.

An additional data set was taken with a  $CH_2$  target  $8 \times 2.6 \times 8$  cm in extent. For this target 44,000 tagged  $K^+$  were found in the reduced data.

### 4. SCINTILLATING FIBER DATA

Scintillating fiber arrays for detecting the decay products of the double hypernucleus are mounted above and below the target as shown in Fig. 1. The arrays are composed of 20,000 1.0 mm fibers in alternate u and v planes viewed by image intensifier tubes (IIT) with a CCD readout. Light output in each fiber is recorded. The scintillating fiber is

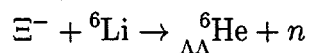
used for study of decay products of hypernuclei and also to help suppress backgrounds.

It may also be possible to observe the sequential two  $\pi^-$  decay of  $\Lambda\Lambda$  hypernuclei (experiment E906 [6] will do this with much higher statistics). It should be pointed out that there will be an angular correlation between these two pions [8]. In  $\Lambda$  decay,  $\pi^-$  are emitted preferentially opposite to the  $\Lambda$  spin direction. For a  $\Lambda\Lambda$  hypernucleus in the ground state, the  $\Lambda$  particles are in a spin-singlet state. Therefore for the sequential decay mode, the pions are more likely to be emitted in opposite directions.

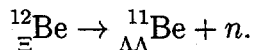
## 5. $\Lambda\Lambda$ HYPERNUCLEI PRODUCED BY $\Xi^-$ CAPTURE

In reaction 1,  $\Xi^-$  capture on carbon results in a  $\Lambda\Lambda$  hypernucleus accompanied by a single neutron; the neutron energy measures the binding energy of the  ${}_{\Lambda\Lambda}^{12}\text{B}$  hypernucleus.

The branching ratio for production of  $\Lambda\Lambda$  hypernuclei accompanied by a single neutron has been calculated in several cases. Zhu and his collaborators [9] have calculated a 5% branching ratio for the reaction



leading to the  ${}_{\Lambda\Lambda}^6\text{He}$  ground state. Millener and his collaborators [10] have calculated a 20% branching ratio for



leading to the  $p_{\Lambda}s_{\Lambda}$  state of  ${}_{\Lambda\Lambda}^{11}\text{Be}$  with the  ${}^9\text{Be}$  core in its ground state. This reaction is similar to our signal reaction in that the neutron energy is 12 MeV; the Q value of the reaction is a major determinant of the lambda sticking probability. Calculations in Ref. [11] obtain a considerably smaller value.

## 6. $\Xi$ HYPERNUCLEI

Except in special cases,  $\Xi$  hypernuclear states will have strong interaction widths since a  $\Xi^-$  can interact with a proton to form two  $\Lambda$  particles.

However, the release of energy is small and can be further reduced by binding effects when the proton is a component of a nucleus. These factors lead to the conclusion that  $\Xi$  hypernuclear states may be narrow. Calculations by Millener [10] and his collaborators, and by Ikeda and his collaborators [12] give  $\approx 1.5$  MeV for the width of these states. Since this is narrow compared to the spacing between states, a spectroscopy may be possible.

We hope to learn from experiment the binding energy of the  $\Xi$  and to deduce the  $\Xi$ -nucleus potential, leading to a greater understanding of the baryon-baryon interaction. Strange hadronic matter [13] will exist only if the  $\Xi$ -nucleus potential is sufficiently strong.

Seven  $\Xi$  hypernuclei candidates reported in emulsion experiments over the period 1959-1969 were analyzed by Dover and Gal in their 1983 review [14]. Typical reported values of  $\Xi$  binding energy were between 10 and 20 MeV for p-shell species. Commenting on the quality of the data they said "none of these interpretations is statistically unique, and in some cases the evidence is far from being compelling". However, using these data they determined the  $\Xi$ -nucleus central potential to be  $V_{0\Xi} \approx 24$  MeV. More recently, a hybrid emulsion experiment found two  $\Xi$  hypernucleus events [15]. These events are superior to the the older emulsion events because they are initiated by an identified  $\Xi^-$

captured at rest; they are consistent with a  $\Xi$  binding energy of less than 4 MeV for the  $\Xi^- - {}^{12}\text{C}$  system. However, there are still multiple interpretations possible for these events.  $\Xi$  hypernuclei could also be detected by a missing mass experiment. KEK E224 has presented low statistics data [16] possibly suggestive of a potential  $V_{0\Xi}$  weaker than 24 MeV.

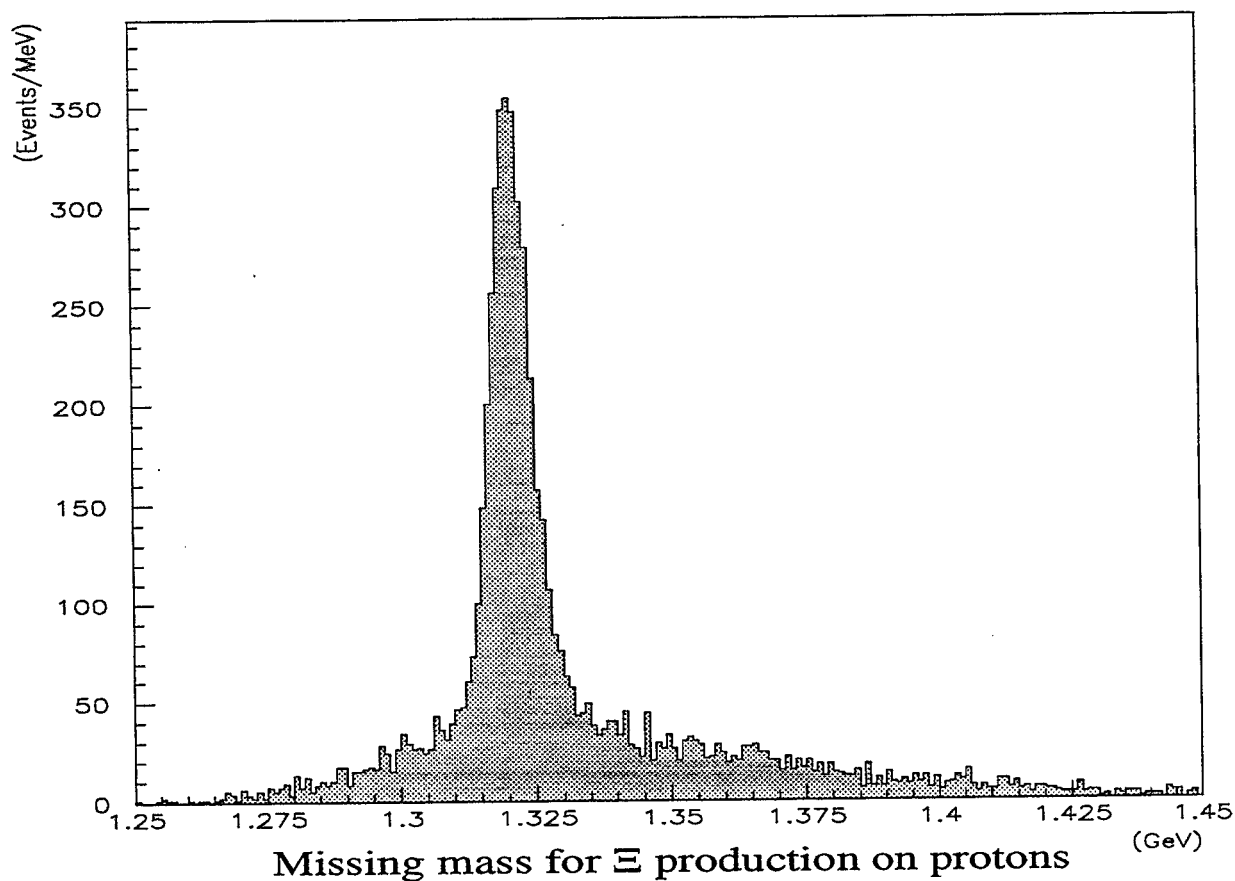


Figure 3. Data taken with the  $\text{CH}_2$  (polyethylene) target plotted with hydrogen kinematics. The horizontal scale is missing mass  $m_X$  in the reaction  $K^- + p \rightarrow X + K^+$ . The peak corresponds to  $\Xi^-$  production on free protons; the continuum, to production on protons bound in  ${}^{12}\text{C}$ .

## 7. ANALYSIS OF THE MISSING MASS SPECTRUM

Analysis of the missing mass spectrum in the reaction  $K^- + {}^{12}\text{C} \rightarrow X + K^+$  can be used in a direct search for  $\Xi$  hypernuclei and also for H particles. The analysis of this section uses only the data taken with the  $\text{CH}_2$  (polyethylene) target by experiment 885; this represents approximately 10% of the total  $(K^-, K^+)$  data on carbon. The presence of free protons in this target makes the analysis straightforward. The narrow peak resulting from

$\Xi^-$  production on free protons (Fig. 3) sets the energy scale, determines the resolution and determines the normalization. For this and other reasons [17], the  $\text{CH}_2$  data are simpler to analyze than the diamond data.

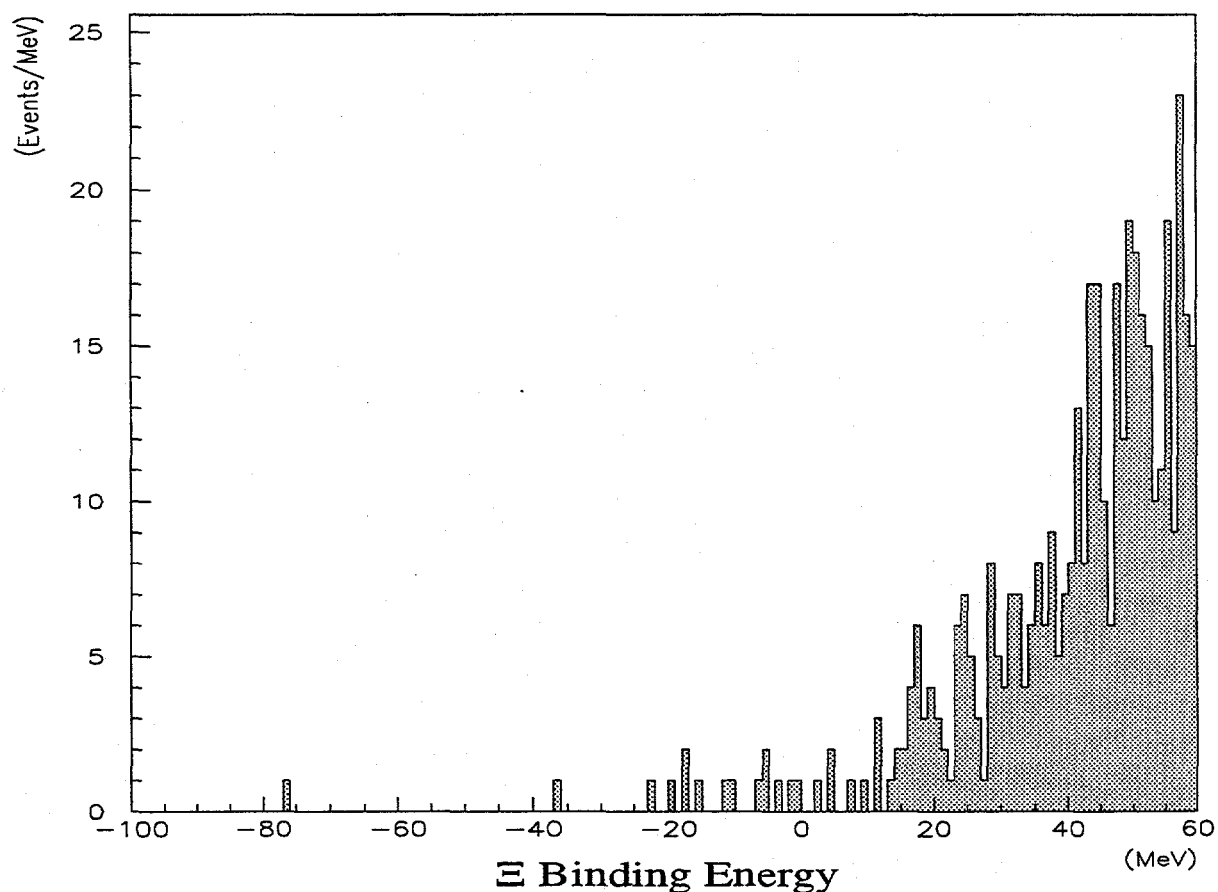


Figure 4.  $\text{CH}_2$  target data plotted with carbon kinematics. The horizontal scale is  $B_{\Xi}$  calculated from missing mass in the reaction  $\text{K}^- + {}^{12}\text{C} \rightarrow \text{X} + \text{K}^+$ .  $B_{\Xi} = 0$  corresponds to a  $\Xi^-$  and  ${}^{11}\text{B}$  just unbound. If events below zero are  $\Xi$  hypernuclei, the species is  ${}^{12}_{\Xi}\text{Be}$ .

Fig. 4 shows the events plotted versus  $\Xi$  binding energy. Zero binding corresponds to production of a  $\Xi^-$  and  ${}^{11}\text{B}$  system just unbound and is fixed by the position of the hydrogen peak in Fig. 3. Events with  $B_{\Xi}$  between 0 and -25 are candidates for  $\Xi$  hypernuclei. The presence of events in this region, and the low background level at more negative values of  $B_{\Xi}$  is intriguing. We are in the process of eliminating possible sources of background and analyzing the large sample of data we have with the diamond target.

The small number of events in the region below -25 MeV indicates that we will also be able to set stringent limits on direct H particle production. Production of an H particle through reaction 3 is expected to result in a peak in the  $\text{K}^+$  momentum spectrum [18].

## REFERENCES

1. R. L. Jaffe, Phys. Rev. Lett. 38 (1977) 195.
2. S. A. Chin and A. K. Kerman, Phys. Rev. Lett. 43 (1979) 1292;  
E. Farhi and R. L. Jaffe, Phys. Rev. D 30 (1984) 2379.
3. E. Witten, Phys. Rev. D 30 (1984) 272; Phys. Rev. D 53 (1996) R3487.
4. M. Danysz et al., Nucl. Phys. 49 (1963) 121;  
D. Prowse, Phys. Rev. Lett. 17 (1966) 782;  
S. Aoki et al., Prog. Theor. Phys. 85 (1991) 1287.
5. AGS Experiment 885 (Brookhaven National Laboratory, Carnegie Mellon University, University of Manitoba, Kyoto University, TRIUMF, University of Freiburg, University of Kentucky, KEK, University of Kyoto Sangyo, LANL, University of New Mexico, Rutgers University), M. May, G. Franklin and C. A. Davis spokesmen. For a list of collaboration members, see the following paper by K. Yamamoto.
6. AGS Experiment 906 (INS-Tokyo, BNL, CMU, Gifu, Freiburg, INR-Russia, Kyoto, Kyoto-Sangyo, Rutgers, TRIUMF, Manitoba, New Mexico), T. Fukuda and R. E. Chrien spokesmen. See the preceding paper by T. Fukuda.
7. K. Imai, private communication.
8. I first became aware of this in a discussion with Maurice Goldhaber. As far as I know it has not previously appeared in the literature.
9. D. Zhu, C. B. Dover, A. Gal and M. May, Phys. Rev. Lett. 67 (1991) 2268.
10. D.J. Millener, C. B. Dover and A. Gal, Prog. Theor. Phys. Suppl. 117 (1994) 307.
11. Y. Yamamoto et al., Prog. Theor. Phys. Suppl. 117 (1994) 281
12. K. Ikeda et al., Prog. Theor. Phys. 91 (1994) 747.
13. J. Schaffner et al., Phys. Rev. Lett. 71 (1993) 1328; Ann. Phys. (N. Y.) 235 (1994) 35.
14. C.B. Dover and A. Gal, Ann. Phys. (N. Y.) 146 (1983) 309.
15. S. Aoki et al., Prog. Theor. Phys. 89 (1993) 493.
16. T. Fukuda et al., in preparation.
17. Because of the narrow vertical size of the the diamond target, some  $K^+$  do not traverse the full target length.
18. A. T. M. Aerts and C. B. Dover, Phys. Rev. D 28 (1983) 450;  
R. W. Stotzer et al., Phys. Rev. Lett. 78 (1997) 3646;  
J. K. Ahn et al., Phys. Lett. B 378 (1996) 53.